Gulf Journal of Mathematics ISSN: 2309-4966
Vol 19, Issue 2 (2025) 181-199 https://doi.org/10.56947/gjom.v19i2.2676

COMPUTATIONAL SPECTRAL METHOD FOR SOLVING TWO-DIMENSIONAL RIESZ MULTI-TERM TIME-FRACTIONAL DIFFUSION EQUATION

MOUHSSINE ZAKARIA[1]* and ABDELAZIZ MOUJAHID[1]

Abstract. This research introduces a spectral element method (SEM) for solving a fractional diffusion model. We propose a discrete-time scheme, using the finite difference method to approach the multi-Caputo fractional derivative on a uniform mesh. In addition, we offer a Galerkin variational formulation to establish the unconditional stability of the scheme. We use the SEM based on Legendre polynomials in the space direction and derive the fully discrete scheme. The error estimation analysis of the fully discrete scheme is proved in the L_2 sense. Finally, we demonstrate the method's effectiveness by numerical experiments and simulations performed in MATLAB.

1. Introduction

Researchers have increasingly focused on solving and analyzing fractional differential equations because they represent a fascinating area of applied mathematics, offering powerful tools to model natural phenomena with memory and hereditary characteristics. These equations have a wide range of applications, warranting further exploration. In physics, [13, 26], and [14] where a fractional Bloch model was utilized to characterize the fundamental processes of nuclear magnetic resonance. In chemistry and biology, the FDEs were able to describe the collective behavior of molecules in transport [22], the transfer of heat and mass [9], and a proposed model of the von Kar-man evolution coupled to the thermoelastic equation [5]. In finance [15], economics [1], and engineering [16]. This development led mathematicians to explore various tools and techniques to simulate their solutions over the years, as finding an analytical solution remains challenging and complex. This has generated a substantial body of research that has significantly contributed to the field, motivating us to explore several of these studies. For example, in [7], the second-order convolution quadrature and the weighted-shifted Grünwald formula were applied to approximate the Riemann–Liouville fractional integral and the distributed-order time fractional derivative, for multidimensional fractional integrodifferential models. Furthermore, the authors employed the energy method to

Date: Received: Feb 4, 2025; Accepted: Mar 2, 2025.
* Corresponding author.
2020 *Mathematics Subject Classification.* Primary 26A33, 35R11, 65M06, 65M12.
Key words and phrases. Fractional diffusion equation(FDE), Caputo and Riesz derivative, Galerkin spectral element method (G-SEM), Legendre polynomials, Stability and Error estimates.

perform an error study for the obtained scheme. The existence and uniqueness were treated via the Banach–Alaoglu theorem in a Sobolev space, for a nonlinear Kortewegde Vries-Rosenau-regularized long-wave problem proposed to model the dynamics of waves propagating in shallow water along lake shores. in [10], and was simulated using the finite element method(FEM) combining with a second-order Crank-Nicolson scheme. The authors designed a finite element analysis to simulate a non-linear advection-diffusion equation in [11], where backward Euler and Crank-Nicolson schemes were used to derive a fully discretization, and the error analysis in Bôchner norms. SEM was created to solve fluid dynamics models, the combination of the FEM and spectral method led to the development of SEM, see [17]. In the literature, SEM is an efficient method to approximate solutions for complex models in applied sciences. In [25], the authors use a non-standard finite difference and an SEM to approach the model. A hybrid SEM is constructed for both Caputo and Riemann-Liouville fractional derivatives to solve fractional two-point boundary value equations. Further, in [12] the authors proposed a numerical method via the SEM and hierarchical matrix approximation to solve an equation with two-sided second-order Riemann-Liouville operators. Studying our model leads to a look at specific studies. For example, Zhao et al. [29], the authors applied the FEM for the one-sided/two-dimensional fractional Bloch–Torrey equation, using the $L2-1_\sigma$ formula to approximate the temporal Caputo derivative, and the FEM to deal with the approximations in the spatial direction leading to a fully discrete scheme solved using linear piecewise polynomials.

This study deals with a finite difference in time and G-SEM in space for a 2D Riesz multi-term time-fractional diffusion equation:

$$\begin{cases} \sum_{s=1}^{l} \mu_s \mathfrak{d}_t^{\alpha_s} \psi(v,w,t) = \Upsilon_1 \frac{\partial^{2\zeta_1}\psi}{\partial|v|^{2\zeta_1}} + \Upsilon_2 \frac{\partial^{2\zeta_2}\psi}{\partial|y|^{2\zeta_2}} + F(v,w,t), \\ \psi(v,w,t) = 0, \quad (v,w,t) \in \partial\Lambda \times (0,T], \\ \psi(v,w,0) = c_{\mathfrak{J}}(v,w), \quad (v,w) \in \Lambda, \end{cases} \tag{1.1}$$

Where $\mu_s, s = 1, \cdots, l$ are given positive parameters. $0 < \alpha_s < 1, s = 1, \cdots, l$. $1 < 2\zeta_1, 2\zeta_2 < 2$, in which $\Lambda = (0,H) \times (0,L) \subset \mathbb{R}^2$, $c_{\mathfrak{J}}$ and F are known smooth functions. And Υ_1, Υ_2 are the non-negative weight coefficients.
The Caputo fractional derivative is define in [18], as follows

$$\mathfrak{d}_t^{\rho}\psi = \frac{1}{\Gamma(n-\rho)} \int_0^t \frac{\psi^{(n)}(v)dv}{(t-v)^{\rho+1-n}}, \quad n-1 < \rho < n, \quad n \in \mathbb{N},$$

with Γ denoting the gamma function. The Riesz fractional derivative on a finite domain [18, 21], is given by:

$$\frac{\partial^{2\kappa}\psi}{\partial|v|^{2\kappa}} = -\frac{1}{2\cos(\kappa\pi)} \left({}_0\mathcal{D}_v^{2\kappa}\psi + {}_v\mathcal{D}_H^{2\kappa}\psi \right),$$

for $n-1 < 2\kappa < n, n \in \mathbb{N}$, the operators ${}_0\mathcal{D}_s^{2\kappa}\psi$, and ${}_s\mathcal{D}_D^{2\kappa}\psi$ are defined as

$$
{}_0\mathcal{D}_s^{2\kappa}\psi = {}_s\mathcal{D}_L^{2\kappa}\psi = \frac{1}{\Gamma(n-2\kappa)}\frac{\partial^n}{\partial s^n}\int_0^s (s-w)^{n-2\kappa-1}\psi(w)dw,
$$
$$
{}_s\mathcal{D}_D^{2\kappa}\psi = {}_s\mathcal{D}_R^{2\kappa}\psi = \frac{(-1)^n}{\Gamma(n-2\kappa)}\frac{\partial^n}{\partial s^n}\int_s^D (w-s)^{n-2\kappa-1}\psi(w)dw.
$$

This paper introduces non-standard procedures for error analysis, utilizing new techniques and results. It presents innovative methods for the analytical study of FDEs. Further, the approach detailing the application of the spectral elements method with Legendre polynomials as the spatial basis. This section offers valuable insights into the implementation process and the numerical solution of the problem using MATLAB software. The rest of the paper is summarized as follows: In section 2, specific backgrounds on fractional spaces are given. In Section 3, the standard L1 formula is applied for time to approximate the multi-Caputo derivative. Further, the unconditional stability for the semi-discrete scheme is established via a Galerkin variational formulation. In Section 4, the spectral element method based on Legendre polynomials is employed in the spatial direction, and we obtain the fully Galerkin spectral element scheme. Next, the convergence analysis of the fully discrete scheme is treated. In Section 5, test problems are presented to validate the effectiveness of the proposed numerical method, supported by simulated graphs. Finally, the essential results are concluded in Section 6.

2. Foundational tools and Backgrounds

To start, we introduce essential concepts and lemmas for theoretical exploration.

2.1. **Fractional spaces: norms and semi-norms.**

We announced some properties concerned with the fractional spaces

Definition 2.1. [20, 6] For $\epsilon > 0$, we introduce the semi-norm and norm, respectively, as follows

$$
|\psi|_{\mathcal{J}_L^\epsilon(\Lambda)} := \left(\|{}_x\mathcal{D}_L^\epsilon\psi\|^2_{L_2(\Lambda)} + \|{}_y\mathcal{D}_L^\epsilon\psi\|^2_{L_2(\Lambda)}\right)^{1/2}, \|\psi\|_{\mathcal{J}_L^\epsilon(\Lambda)} := \left(\|\psi\|^2_{L_2(\Lambda)} + |\psi|^2_{\mathcal{J}_L^\epsilon(\Lambda)}\right)^{1/2},
$$

and denote $\mathcal{J}_L^\epsilon(\Lambda)(\mathcal{J}_{L,0}^\epsilon(\Lambda))$ as the closure of $C^\infty(\Lambda)(C_0^\infty(\Lambda))$ with respect to $\|\cdot\|_{\mathcal{J}_L^\epsilon(\Lambda)}$

Definition 2.2. [20, 6] For $\epsilon > 0$, we introduce the semi-norm and norm, respectively, as follows.

$$
|\psi|_{\mathcal{J}_R^\epsilon(\Lambda)} := \left(\|{}_x\mathcal{D}_R^\epsilon\psi\|^2_{L_2(\Lambda)} + \|{}_y\mathcal{D}_R^\epsilon\psi\|^2_{L_2(\Lambda)}\right)^{1/2}, \|\psi\|_{\mathcal{J}_R^\epsilon(\Lambda)} := \left(\|\psi\|^2_{L_2(\Lambda)} + |\psi|^2_{\mathcal{J}_R^\epsilon(\Lambda)}\right)^{1/2},
$$

and denote $\mathcal{J}_R^\epsilon(\Lambda)(\mathcal{J}_{R,0}^\epsilon(\Lambda))$ as the closure of $C^\infty(\Lambda)(C_0^\infty(\Lambda))$ with respect to $\|\cdot\|_{\mathcal{J}_R^\epsilon(\Lambda)}$.

Definition 2.3. [20, 6] For $\epsilon > 0, \epsilon \neq n - \frac{1}{2}, n \in \mathbb{N}$, we introduce the semi-norm and norm, respectively, as follows.

$$
|\psi|_{\mathcal{J}_S^\epsilon(\Lambda)} = \left(|({}_x\mathcal{D}_L^\epsilon\psi, {}_x\mathcal{D}_R^\epsilon\psi)| + |({}_y\mathcal{D}_L^\epsilon\psi, y\mathcal{D}_R^\epsilon\psi)|\right)^{1/2}, \|\psi\|_{\mathcal{J}_S^\epsilon(\Lambda)} := \left(\|\psi\|^2_{L_2(\Lambda)} + |\psi|^2_{\mathcal{J}_S^\epsilon(\Lambda)}\right)^{1/2}
$$

and denote $\mathcal{J}_S^\epsilon(\Lambda)(\mathcal{J}_{S,0}^\epsilon(\Lambda))$ as the closure of $C^\infty(\Lambda)(C_0^\infty(\Lambda))$ with respect to $\|\cdot\|_S^\epsilon(\Lambda)$.

Definition 2.4. [20, 6] For $\epsilon > 0$, we introduce the semi-norm and norm, respectively, as follows.

$$|\psi|_{\mathcal{H}^\epsilon(\Lambda)} := \left\| |z|^\epsilon \mathcal{F}(\hat{\Theta})(z) \right\|_{L_2(\Lambda)}, \|\psi\|_{\mathcal{H}^\epsilon(\Lambda)} := \left(\|\psi\|^2_{L_2(\Lambda)} + |\psi|^2_{\mathcal{H}^\epsilon(\Lambda)} \right)^{1/2},$$

where $\mathcal{F}(\hat{\psi})(z)$ is the Fourier transform of $\hat{\psi}$ and $\hat{\psi}$ is the zero extension of ψ outside Λ, and denote $\mathcal{H}^\epsilon(\Lambda)\,(\mathcal{H}_0^\epsilon(\Lambda))$ as the closure of $C^\infty(\Lambda)\,(C_0^\infty(\Lambda))$ with respect to $\|\cdot\|_{\mathcal{H}^\epsilon(\Lambda)}$.

Definition 2.5. [20, 6] We define the spaces $\mathcal{J}_{L,0}^\epsilon(\Lambda), \mathcal{J}_{R,0}^\epsilon(\Lambda), \mathcal{J}_{S,0}^\epsilon(\Lambda)$ and $\mathcal{H}_0^\epsilon(\Lambda)$ with respect to related norms, as the closer of $C_0^\infty(\Lambda)$.

Lemma 2.6. [20] *Let $\epsilon > 0, \psi^n \in \mathcal{J}_{L,0}^\epsilon \cap \mathcal{J}_{R,0}^\epsilon$, therefore*

$$({}_x\mathcal{D}_L^\epsilon \psi, {}_x\mathcal{D}_R^\epsilon \psi)_{L^2(\Lambda)} = \left({}_x\mathcal{D}_L^\epsilon \hat{\psi}, {}_x\mathcal{D}_R^\epsilon \hat{\psi} \right)_{L^2(\mathbb{R}^2)} = \cos(\epsilon\pi) \left\| {}_x\mathcal{D}_L^\epsilon \hat{\psi} \right\|_{L^2(\mathbb{R}^2)}$$
$$({}_y\mathcal{D}_L^\epsilon \psi, {}_y\mathcal{D}_R^\epsilon \psi)_{L^2(\Lambda)} = \left({}_y\mathcal{D}_L^\epsilon \hat{\psi}, {}_y\mathcal{D}_R^\epsilon \hat{\psi} \right)_{L^2(\mathbb{R}^2)} = \cos(\epsilon\pi) \left\| {}_y\mathcal{D}_L^\epsilon \hat{\psi} \right\|_{L^2(\mathbb{R}^2)},$$

Where $\hat{\psi}$ is the zero extension of ψ outside Λ.

Lemma 2.7. [20, 6] *For all $\epsilon > 0$, the spaces $\mathcal{J}_L^\epsilon(\mathbb{R}^2), \mathcal{J}_R^\epsilon(\mathbb{R}^2), \mathcal{J}_S^\epsilon(\mathbb{R}^2)$ and $\mathcal{H}^\epsilon(\mathbb{R}^2)$ are equal with respected semi-norms and norms. For $\epsilon > 0, \epsilon \neq n - \frac{1}{2}, n \in \mathbb{N}$, spaces $\mathcal{J}_{L,0}^\epsilon(\Lambda), \mathcal{J}_{R,0}^\epsilon(\Lambda), \mathcal{J}_{S,0}^\epsilon(\Lambda)$ and $\mathcal{H}_0^\epsilon(\Lambda)$ are equal with respected semi-norms and norms.*

Lemma 2.8. [20, 6] *For $\psi \in \mathcal{J}_{L,0}^\epsilon(\Lambda), 0 < p < \epsilon$ then, there exist a reels $\mathcal{C}_q, \mathcal{C} > 0$ and $\mathcal{C}_i > 0, i = 1, 2, 3, 4$*

$$\|\psi\|_{L^2(\Lambda)} \le \mathcal{C}|\psi|_{\mathcal{J}_L^\epsilon(\Lambda)}, \quad |\psi|_{\mathcal{J}_L^\epsilon(\Lambda)} \le \mathcal{C}|\psi|_{\mathcal{J}_L^\epsilon(\Lambda)}, \|\psi\|_{\mathcal{J}_L^\epsilon(\Lambda)} \le \mathcal{C}_q|\psi|_{\mathcal{J}_L^\epsilon(\Lambda)},$$
$$\|\psi\|_{L^2(\Lambda)} \le \mathcal{C}_1 \left\| {}_x\mathcal{D}_L^p \psi \right\|_{L^2(\Lambda)} \le \mathcal{C}_2 \left\| {}_x\mathcal{D}_L^\epsilon \psi \right\|_{L^2(\Lambda)},$$
$$\|\psi\|_{L^2(\Lambda)} \le \mathcal{C}_3 \left\| {}_y\mathcal{D}_L^p \psi \right\|_{L^2(\Lambda)} \le \mathcal{C}_4 \left\| {}_y\mathcal{D}_L^\epsilon \psi \right\|_{L^2(\Lambda)},$$

In the same way, the results mentioned above apply to the spaces. $\mathcal{J}_{R,0}^\epsilon(\Lambda), \mathcal{J}_{S,0}^\epsilon(\Lambda)$ and $\mathcal{H}_0^\epsilon(\Lambda)\left(v \neq n - \frac{1}{2}\right)$.

Lemma 2.9. [20, 6] *If $\epsilon \in (0, 1), v, w \in \mathcal{J}_L^{2\epsilon}(\Lambda)$, and, $v|_{\partial\Lambda} = 0$, and $w|_{\partial\Lambda} = 0$, then*

$$\left({}_x\mathcal{D}_R^{2\epsilon} v, w \right) = \left({}_x\mathcal{D}_R^\epsilon v, {}_x\mathcal{D}_L^\epsilon w \right), \quad \left({}_y\mathcal{D}_L^{2\epsilon} v, w \right) = \left({}_y\mathcal{D}_L^\epsilon v, {}_y\mathcal{D}_R^\epsilon w \right),$$
$$\left({}_y\mathcal{D}_R^{2\epsilon} v, w \right) = \left({}_y\mathcal{D}_R^\epsilon v, {}_y\mathcal{D}_L^\epsilon w \right), \quad \left({}_y\mathcal{D}_L^{2\epsilon} v, w \right) = \left({}_y\mathcal{D}_L^\epsilon v, {}_y\mathcal{D}_R^\epsilon w \right).$$

Lemma 2.10. [19] *(Discrete Gronwall Inequality). Let U_m denote a non-negative sequence, and let the sequence q_m satisfy*

$$\begin{cases} q_0 \le p_0, \\ q_m \le p_0 + \sum_{i=0}^{m-1} s_i + \sum_{i=0}^{m-1} U_i q_i, \quad m \ge 1, \end{cases}$$

If $p_0 \geq 0$ and $s_0 \geq 0$, we have

$$q_m \leq \left(p_0 + \sum_{i=0}^{m-1} s_i\right) \exp\left(\sum_{i=0}^{m-1} U_i\right), \quad m \geq 1.$$

3. Construction of the time-discrete scheme

We will use the Crank-Nicolson approach in the temporal direction. Let $\Delta t = \frac{T}{\mathcal{N}}$ be the time step and $t_n = n\Delta t$ such that $n = 0, 1, \ldots, \mathcal{N}, \mathcal{N} \in \mathbb{N}^+$. For $\psi \in C(\Lambda \times [0, T])$, we consider $\psi^n(\cdot) = \psi(\cdot, t_n)$.

To approximate the fractional Caputo derivative, we bring to the standard L1 formula on a uniform mesh, then ${}^c\mathfrak{d}_t^{\alpha_s}\psi(t)$ at $t = t_n$, for $n = 1, 2, \cdots, \mathcal{N}$ can be approximated by

$$\mathfrak{D}_t^{\alpha_s}\psi^n = \frac{1}{\Gamma(2-\alpha_s)}\left[p_1^s\psi^n + \sum_{i=1}^{n-1}\left(p_{i+1}^s - p_i^s\right)\psi^{n-i} - p_n^s\psi^0\right] = \frac{\Delta t^{-\alpha_s}}{\Gamma(2-\alpha_s)}\sum_{i=0}^{n} d_i^s\psi^i,$$

$$\text{where} \quad \Delta t^{-\alpha_s} d_{n-i}^s = p_{i+1}^s - p_i^s, \quad 1 \leq i \leq n-1, \quad -\sum_{i=0}^{n-1} d_i^s = d_n^s \quad 1 \leq s \leq l, \tag{3.1}$$

$$\Delta t^{-\alpha_s} d_0^s = -p_n^s, \quad d_n^s = 1, \quad \textit{and} \quad p_i^s = \frac{(t_n - t_{n-i})^{1-\alpha_s} - (t_n - t_{n-i+1})^{1-\alpha_s}}{\Delta t}, \quad i \geq 1,$$

We can get via the mean value theorem, that

$$\Delta t^{-\alpha_s} = p_1^s \leq p_i^s \leq p_{i+1}^s, \quad i \geq 2. \tag{3.2}$$

Lemma 3.1. [27] *Let $\psi \in C^2(0, T] \bigcap C(0, T]$, suppose $\left|\frac{d^p\psi}{dt}\right| \leq C_1\left(1 + t^{\eta - l}\right)$ for $p = 0, 1, 2$ and $0 < \eta < 1$, then there exists C_2, where the truncation error of the L1 formula (3.1) satisfies*

$$\left|\mathfrak{R}_\eta^n\right| = \left|\mathfrak{d}_t^\eta\psi(t_n) - \mathfrak{D}_t^\eta\psi(t_n)\right| \leq C_2\Delta t^{2-\eta}.$$

Building on the previous results, the multi-term Caputo fractional derivative can be approximated as:

$$\mathcal{T}_t\psi(t_n) = \sum_{s=0}^{l}\mathfrak{D}_t^{\gamma_s}\psi(t_n) = \xi_1\psi^n + \sum_{i=1}^{n-1}\left(\xi_{i+1} - \xi_i\right)\psi^{n-i} - \xi_n\psi^0,$$

where $\xi_i = \sum_{s=1}^{l}\frac{\mu_s p_i^s}{\Gamma(2-\alpha_s)}$, for $i = 1, \ldots, N$. Further, there exist α, where the truncation error $\mathfrak{R}^n$ verifies

$$|\mathfrak{R}^n| = \left|\sum_{s=0}^{l}\mu_s\mathfrak{R}_{\alpha_s}^n\right| \leq e\sum_{s=0}^{l}\mu_s\Delta t^{2-\alpha_s} \leq e\Delta t^{2-\alpha}$$

We conclude the discrete scheme in the time direction at the point. $t = t_n$ as

$$\mathcal{T}_t\psi^n = \Upsilon_1\frac{\partial^{2\zeta_1}\psi^n}{\partial|x|^{2\zeta_1}} + \Upsilon_2\frac{\partial^{2\zeta_2}\psi^n}{\partial|y|^{2\zeta_2}} + F^n + \mathfrak{R}^n, \tag{3.3}$$

Eliminating the small term $\mathfrak{R}^n$, we have

$$\mathcal{T}_t\bar{\psi}^n = \Upsilon_1 \frac{\partial^{2\zeta_1}\bar{\psi}^n}{\partial|x|^{2\zeta_1}} + \Upsilon_2 \frac{\partial^{2\zeta_2}\bar{\psi}^n}{\partial|y|^{2\zeta_2}} + F^n, \tag{3.4}$$

The Galerkin variational formulation of (3.4), shown as find $\bar{\psi}^n \in \mathcal{H}_0^{\zeta_1} \cap \mathcal{H}_0^{\zeta_2}$ verified

$$\left(\mathcal{T}_t\bar{\psi}^n, e\right) + \mathcal{A}\left(\bar{\psi}^n, e\right) = \left(F^n, e\right), \quad \forall e \in \mathcal{H}_0^{\zeta_1} \cap \mathcal{H}_0^{\zeta_2}, \tag{3.5}$$

where $\mathcal{A}$ can expressed as

$$\begin{aligned}\mathcal{A}(v,w) = {} & \frac{\Upsilon_1}{2\cos(\zeta_1\pi)}\left[\left({}_x\mathcal{D}_L^{\zeta_1}v, {}_x\mathcal{D}_R^{\zeta_1}w\right) + \left({}_x\mathcal{D}_R^{\zeta_1}v, {}_x\mathcal{D}_L^{\zeta_1}w\right)\right] \\ & + \frac{\Upsilon_2}{2\cos(\zeta_2\pi)}\left[\left({}_y\mathcal{D}_L^{\zeta_2}v, {}_y\mathcal{D}_R^{\zeta_2}w\right) + \left({}_y\mathcal{D}_R^{\zeta_2}v, {}_y\mathcal{D}_L^{\zeta_2}w\right)\right].\end{aligned}$$

Theorem 3.2. *For $\bar{\psi}^n \in \mathcal{H}_0^{\zeta_1} \cap \mathcal{H}_0^{\zeta_2}$ solution of the time discrete scheme (3.5) there exists $\mathcal{M}_1$, $\mathcal{M}_2 > 0$, where we have the following estimation,*

$$\left\|\bar{\psi}^n\right\|_{L^2(\Lambda)} \le \mathcal{M}_1 \left\|\bar{\psi}^0\right\|_{L^2(\Lambda)} + \mathcal{M}_2 \max_{0\le j\le n}\left\|F^j\right\|_{L^2(\Lambda)}.$$

Proof. Replacing $e = \bar{\psi}^n$ in Eq.(3.5), we obtain

$$\left(\mathcal{T}_t\bar{\psi}^n, \bar{\psi}^n\right) + \mathcal{A}\left(\bar{\psi}^n, \bar{\psi}^n\right) = \left(F^n, \bar{\psi}^n\right), \tag{3.6}$$

According to Lemma 2.6, $\mathcal{A}\left(\bar{\psi}^n, \bar{\psi}^n\right) \ge 0$, then

$$\xi_1\left\|\bar{\psi}^n\right\|^2_{L^2(\Lambda)} \le \xi_n(\bar{\psi}^0, \bar{\psi}^n) - \sum_{i=1}^{n-1}\left(\xi_{i+1} - \xi_i\right)\left(\bar{\psi}^{n-i}, \bar{\psi}^n\right) + \left(F^n, \bar{\psi}^n\right),$$

Via (3.2), and using the Cauchy-Schwarz, Young inequality, we get

$$\xi_1^s\left\|\bar{\psi}^n\right\|_{L^2(\Lambda)} \le \xi_n^s\left\|\bar{\psi}^0\right\|_{L^2(\Lambda)} + \sum_{i=1}^{n-1}\left(\xi_i - \xi_{i+1}\right)\left\|\bar{\psi}^{n-i}\right\|_{L^2(\Lambda)} + \left\|F^n\right\|_{L^2(\Lambda)},$$

which implies that

$$\left\|\bar{\psi}^n\right\|_{L^2(\Lambda)} \le \frac{\xi_n}{\xi_1}\left\|\bar{\psi}^0\right\|_{L^2(\Lambda)} - \frac{1}{\xi_1}\sum_{i=1}^{n-1}\left(\xi_{n-i} - \xi_{n-i+1}\right)\left\|\bar{\psi}^{n-i}\right\|_{L^2(\Lambda)} + \frac{1}{\xi_1}\left\|F^n\right\|_{L^2(\Lambda)},$$

According to (3.2) and Lemma 2.10, we obtain

$$\left\|\bar{\psi}^n\right\|_{L^2(\Lambda)} \le \frac{1}{\xi_1}\left(\xi_n\left\|\bar{\psi}^0\right\|_{L^2(\Lambda)} + \left\|F^n\right\|_{L^2(\Lambda)}\right)\exp\left(\frac{1}{\xi_1}\sum_{i=1}^{n-1}\left(\xi_{n-i} - \xi_{n-i+1}\right)\right),$$

we obtain

$$\left\|\bar{\psi}^n\right\|_{L^2(\Lambda)} \le \frac{1}{\xi_1}\exp\left(\frac{1}{\xi_1}\left(\xi_1^s - \xi_n\right)\right)\left(\xi_n\left\|\bar{\psi}^0\right\|_{L^2(\Lambda)} + \left\|F^n\right\|_{L^2(\Lambda)}\right), \tag{3.7}$$

Using the mean value theorem, we get

$$\frac{1}{\xi_1}\left(\xi_1-\xi_n\right)=\frac{\sum_{s=1}^{l}\frac{\mu_s\Delta t^{-\alpha_s}}{\Gamma(2-\alpha_s)}(1-n^{1-\alpha_s}+(n-1)^{1-\alpha_s})}{\sum_{s=1}^{l}\frac{\mu_s\Delta t^{-\alpha_s}}{\Gamma(2-\alpha_s)}}\leq 1, \tag{3.8}$$

$$\frac{1}{\xi_1}\leq M_1\Delta t^{\alpha_{\max}}, \quad \text{and} \qquad \frac{\xi_n}{\xi_1}\leq\frac{\sum_{s=1}^{l}\frac{\mu_s\Delta t^{-\alpha_s}}{\Gamma(2-\alpha_s)}(1-\alpha_s)}{\sum_{s=1}^{l}\frac{\mu_s\Delta t^{-\alpha_s}}{\Gamma(2-\alpha_s)}}\leq M_2\left(1-\alpha_{\min}\right), \tag{3.9}$$

Where $\alpha_{\min}=\min\left(\alpha\right)_{s=1,\cdots,l.}$, and $\alpha_{\max}=\max\left(\alpha\right)_{s=1,\cdots,l.}$

Applying (3.8) and (3.9) to (3.7), we conclude that

$$\left\|\bar{\psi}^n\right\|_{L^2(\Lambda)}\leq M_2\exp(1)(1-\alpha_{\min})\left\|\bar{\psi}^0\right\|_{L^2(\Lambda)}+M_1\exp(1)T^{\alpha_{\max}}\max_{0\leq j\leq n}\left\|F^j\right\|_{L^2(\Lambda)}.$$

The proof is completed.

4. The G-SEM analysis

This section focuses on the process of the spectral element method and studies convergence analysis.

4.1. **Legendre polynomials formulas.** We now announced a collection of fundamental formulas for Legendre polynomials [23, 24]. The Legendre polynomials $\mathcal{L}_p(x), p=0,1,\ldots,$ are the eigenfunctions of the singular Sturm-Liouville problem:

$$\left(\left(1-x^2\right)\mathcal{L}_n'(x)\right)'+\lambda_n\mathcal{L}_n(x)=0, \quad \lambda_n=n(n+1),$$

or equivalently

$$\left(1-x^2\right)\mathcal{L}_n''(x)-2x\mathcal{L}_n'(x)+n(n+1)\mathcal{L}_n(x)=0.$$

If $\mathcal{L}_n(x)$ is normalized so that $\mathcal{L}_n(1)=1$, then the Legendre polynomials has the following expansion:

$$\mathcal{L}_n(x)=\frac{1}{2^n}\sum_{i=0}^{[n/2]}(-1)^i\binom{n}{i}\binom{2n-2i}{n}x^{n-2i}, \qquad n\geq 0,$$

where $[n/2]$ denotes the integral part of $n/2$. The Legendre polynomials satisfy the three-term recurrence relation and Rodrigues' formula, respectively:

$$\mathcal{L}_{n+1}(x)=\frac{2n+1}{n+1}x\mathcal{L}_n(x)-\frac{n}{n+1}\mathcal{L}_{n-1}(x), \quad \mathcal{L}_n(x)=\frac{1}{2^n n!}\frac{d^n}{dx^n}\left[\left(x^2-1\right)^n\right], \quad n\geq 0,$$

where the first few Legendre polynomials are:

$$\mathcal{L}_0(x)=1, \quad \mathcal{L}_1(x)=x, \quad \mathcal{L}_2(x)=\frac{1}{2}\left(3x^2-1\right), \quad \mathcal{L}_3(x)=\frac{1}{2}\left(5x^3-3x\right).$$

4.2. **The fully discrete scheme.** The challenge in implementing the G-SEM lies in calculating the bilinear form $\mathcal{A}(\psi_n,\xi)$, this leads us to evaluate $({}_x\mathcal{D}_R^{2\beta}X_n,\xi)$ and $({}_x\mathcal{D}_R^{2\beta}X_n,\xi)$, let $m=1,2.$, and $m-1<2\beta<m$. We will divide the domain into non-overlapping K elements. First, we announced the following lemmas.

Lemma 4.1. [24] *Let us represent* $q_n=\frac{1}{\sqrt{4n+6}},\quad \phi_n(x)=q_n\left(\mathcal{L}_n(x)-\mathcal{L}_{n+2}(x)\right),$ $1\le x\le -1,$

$$\mathbf{b}_{in}=\int_{-1}^{1}\left(\phi_n(x),\phi_i(x)\right)dx,\quad \textit{then}\qquad \mathbf{b}_{in}=\mathbf{b}_{ni}=\begin{cases} q_nq_i\left(\frac{2}{2i+1}+\frac{2}{2i+5}\right), & n=i\\ -q_nq_i\frac{2}{2n+1}, & n=i+2\\ 0, & \textit{Otherwise}\ .\end{cases}$$

Lemma 4.2. [8] *For all $\beta>0$, we have*

$$ {}_{-1}\mathcal{D}_w^{\beta}\mathcal{L}_j(w)=\frac{\Gamma(j+1)}{\Gamma(j-\beta+1)}(1+w)^{-\beta}\mathcal{J}_j^{\beta,-\beta}(w),\quad -1\le w\le 1,$$
$$ {}_{w}\mathcal{D}_1^{\beta}\mathcal{L}_j(w)=\frac{\Gamma(j+1)}{\Gamma(j-\beta+1)}(1-w)^{-\delta}\mathcal{J}_j^{\beta,-\beta}(w),\quad -1\le w\le 1,$$

where $\mathcal{J}_j^{\beta_1,\beta_2}(w),(\beta_1,\beta_2>-1)$ are Jacobi polynomial.

For the 1D case, we give the approximation of the solution ψ^n as:

$$\psi\left(x,t_n\right)=\sum_{j=0}^{N}\psi\left(x_j,t_n\right)\phi_j(x),\quad n=1,2,\cdots,\mathcal{N}.$$

So then we compute $\left({}_x\mathfrak{D}_L^{2\eta}\theta^n,\xi\right)$ and $\left({}_x\mathfrak{D}_R^{2\eta}\theta^n,\xi\right)$ as follow

$$\left({}_x\mathcal{D}_L^{2\beta}\psi^n,\xi\right)=\sum_{e=1}^{K}\left({}_x\mathcal{D}_L^{2\beta}\psi^n,\xi\right)_{\Lambda_e}$$
$$=\sum_{e=1}^{K}\left(\sum_{q=1}^{e-1}\int_{\Lambda e}\frac{1}{\Gamma(m-2\beta)}\frac{d^m}{dx^m}\int_{x_{q-1}}^{x_q}(x-\rho)^{m-2\beta-1}\psi^n(\rho)d\rho\xi d\Lambda_e+\left({}_{x_{e-1}}\mathcal{D}_x^{2\beta}\psi^n,\xi\right)_{\Lambda_e}\right)$$
$$=\sum_{e=1}^{K}\left(\sum_{q=1}^{e-1}\int_{\Lambda e}\frac{1}{\Gamma(m-2\beta)}\frac{d^m}{dx^m}\int_{x_{q-1}}^{x_q}(x-\rho)^{m-2\beta-1}\psi^n(\rho)d\rho\xi d\Lambda_e+\left({}_{x_{e-1}}\mathcal{D}_x^{\beta}\psi^n,{}_x\mathcal{D}_{x_e}^{\beta}\xi\right)_{\Lambda_e}\right),$$

and

$$\left({}_x\mathcal{D}_R^{2\beta}\psi^n,\xi\right)=\sum_{e=1}^{K}\left({}_x\mathcal{D}_R^{2\beta}\psi^n,\xi\right)_{\Lambda_e}$$
$$=\sum_{e=1}^{K}\left(\left({}_x\mathcal{D}_{x_e}^{2\beta}\psi^n,\xi\right)_{\Lambda_e}+\sum_{u=e+1}^{K}\int_{\Lambda e}\frac{(-1)^m}{\Gamma(m-2\beta)}\frac{d^m}{dx^m}\int_{x_{u-1}}^{x_u}(\rho-x)^{m-2\beta-1}\psi^n(\rho)d\rho\xi d\Lambda_e\right)$$
$$=\sum_{e=1}^{K}\left(\left({}_x\mathcal{D}_{x_e}^{\beta}\psi^n,{}_{x_{e-1}}\mathcal{D}_x^{\beta}\xi\right)_{\Lambda_e}+\sum_{u=e+1}^{K}\int_{\Lambda e}\frac{(-1)^m}{\Gamma(m-2\beta)}\frac{d^m}{dx^m}\times\int_{x_{u-1}}^{x_u}(\rho-x)^{m-2\beta-1}\psi^n(\rho)d\rho\xi d\Lambda_e\right).$$

As a result, we need to calculate $\left({}_{x_{e-1}}\mathcal{D}_x^{\beta}\mathcal{L}_j(w),{}_x\mathcal{D}_{x_e}^{\beta}\mathcal{L}_k(w)\right)_{\Lambda_e}$

As in [4], for $h_e=x_e-x_{e-1}$ be the length of the element e, then the map function from the e into $[-1,1]$, and its inverse can be given by

$$x(z)=\frac{1}{2}\left[\left(x_e-x_{e-1}\right)z+\left(x_e+x_{e-1}\right)\right],\quad -1\leq z\leq 1,\quad z(x)=\frac{2}{h_e}\left(x-x_{e-1}\right)-1,$$

Therefore, we have

$$\mathbf{b}_{ip}^{e}=\int_{x_{e-1}}^{x_e}\psi_i(x)\psi_p(x)dx=\frac{h_e}{2}\int_{-1}^{1}\psi_i(z)\psi_p(z)dz,$$

then we obtain

$${}_{x_{e-1}}\mathcal{D}_x^{\beta}\mathcal{L}_i(w)=\frac{1}{\Gamma(1-\beta)}\frac{d}{dx}\int_{x_{e-1}}^{x}(x-s)^{-\beta}\mathcal{L}_i(\hat{s})ds=\left(\frac{h_e}{2}\right)^{-\beta}{}_{-1}\mathcal{D}_{\mu}^{\beta}\mathcal{L}_i(w),\quad 0<\beta<1$$

$${}_{x}\mathcal{D}_{x_e}^{\beta}\mathcal{L}_i(w)=\frac{-1}{\Gamma(1-\beta)}\frac{d}{dx}\int_{x}^{x_e}(s-x)^{-\beta}\mathcal{L}_i(\hat{s})ds=\left(\frac{h_e}{2}\right)^{-\beta}{}_{w}\mathcal{D}_{1}^{\beta}\mathcal{L}_i(w),\quad 0<\beta<1$$

where $-1\leq\hat{s}\leq 1$. that gives

$$\begin{aligned}
&\left({}_{x_{e-1}}\mathcal{D}_x^{\beta}\mathcal{L}_j(w),{}_{x}\mathcal{D}_{x_e}^{\beta}\mathcal{L}_k(w)\right)_{\Lambda_e}\\
&=\int_{x_{e-1}}^{x_e}{}_{x_{e-1}}\mathcal{D}_x^{\beta}\mathcal{L}_j(w){}_{x}\mathcal{D}_{x_e}^{\beta}\mathcal{L}_k(w)dx=\left(\frac{h_e}{2}\right)^{1-2\beta}\int_{-1}^{1}{}_{-1}\mathcal{D}_w^{\beta}\mathcal{L}_j(w){}_{w}\mathcal{D}_1^{\beta}\mathcal{L}_k(w)dw\\
&=\left(\frac{h_e}{2}\right)^{1-2\beta}\frac{\Gamma(j+1)}{\Gamma(j-\beta+1)}\frac{\Gamma(k+1)}{\Gamma(k-\beta+1)}\int_{-1}^{1}(1+w)^{-\beta}(1-w)^{\beta}\mathcal{J}_j^{\beta,-\beta}\mathcal{J}_k^{-\beta,\beta}dw\\
&=\left(\frac{h_e}{2}\right)^{1-2\beta}\frac{\Gamma(j+1)}{\Gamma(j-\beta+1)}\frac{\Gamma(k+1)}{\Gamma(k-\beta+1)}\sum_{l=0}^{N}\mathcal{W}_l\mathcal{J}_j^{\beta,-\beta}\left(w_l\right)\mathcal{J}_k^{-\beta,\beta}\left(w_l\right).
\end{aligned}$$

where $\{\mathcal{W}_l\}_{l=0}^{N}$ are the weights functions and $\{w_l\}_{l=0}^{N}$ are the Jacobi-Gauss-Lobatto quadrature, [23].

In the 2D case, we give the approximation of the solution θ^n as:

$$\psi^n\left(x,y,t_n\right)=\sum_{i=0}^{N}\sum_{j=0}^{N}\psi^n\left(x_i,y_j,t_n\right)\phi_i(x)\phi_j(y),\quad 1\leq n\leq\mathcal{N}$$

The chosen basis consists of polynomials of order N, and the element matrices are given by

$$\begin{aligned}
&\mathbf{b}^{Qe}=\mathbf{b}_x\otimes\mathbf{b}_y,\qquad \mathbf{D}_{lx}^{Qe}=\mathbf{D}_{lx}^{e}\otimes\mathbf{b}_y,\quad \mathbf{D}_{rx}^{Qe}=\mathbf{D}_{rx}^{e}\otimes\mathbf{b}_y,\\
&\mathbf{G}_x^{Qel}=\mathbf{G}_x^{el}\otimes\mathbf{b}_y,\quad \mathbf{L}_x^{Qer}=\mathbf{L}_x^{er}\otimes\mathbf{b}_y.
\end{aligned}$$

Where

$$\left(\mathbf{D}_{lx}^{e}\right)_{ij}=\int_{x_{e-1}}^{x_e}{}_{x_{e-1}}\mathcal{D}_x^{\beta}\phi_j^{(e)}(x){}_{x}\mathcal{D}_{x_e}^{\beta}\phi_i^{(e)}(x)dx,\quad \left(\mathbf{D}_{rx}^{e}\right)_{ij}=\int_{x_{e-1}}^{x_e}{}_{x}\mathcal{D}_{x_e}^{\beta}\phi_j^{(e)}(x){}_{x_{e-1}}\mathcal{D}_x^{\beta}\phi_i^{(e)}(x)dx,$$

$$\left(\mathbf{G}_x^{el}\right)_{ij}=\int_{x_{e-1}}^{x_e}\frac{1}{\Gamma(m-2\beta)}\frac{d^m}{dx^m}\int_{x_{l-1}}^{x_l}(x-s)^{m-2\beta-1}\phi_j^{(l)}(s)ds\phi_i^{(e)}(x)dx,$$

$$\left(\mathbf{L}_x^{er}\right)_{ij}=\int_{x_{e-1}}^{x_e}\frac{(-1)^m}{\Gamma(m-2\beta)}\frac{d^m}{dx^m}\int_{x_{r-1}}^{x_r}(s-x)^{m-2\beta-1}\phi_j^{(r)}(s)ds\phi_i^{(e)}(x)dx.$$

Using the integration by parts recursively, we can directly calculate $\mathbf{G}^{el}$ and $\mathbf{L}^{er}$.

The same procedure is used to calculate $({}_y\mathcal{D}_R^{2\beta}\psi_n,\xi)$ and $({}_y\mathcal{D}_R^{2\beta}\psi_n,\xi)$, also to derive the element matrices.

4.3. **Convergence analysis.** This subsection traits the error analysis of the fully Galerkin spectral element method. for that, we declare for some notions and lemmas. $(\|\cdot\|_{L_2(\Lambda)}=\|\cdot\|)$

We define the space $\mathcal{W}_h^0$ as

$$\mathcal{W}_h^0=\left\{v\in\mathcal{H}_0^{\zeta_1}\cap\mathcal{H}_0^{\zeta_2}:v|_{\Lambda_e}\in\mathbf{P}_N\right\}.$$

where $\mathbf{P}_N$ is the space of polynomials of degree no more than $N\in\mathbb{N}$.

Let $\mathcal{Q}_h^{\zeta_1,\zeta_2,0}$ be the orthogonal projection operator, map from $\mathcal{H}_0^{\zeta}(\Lambda)\cap\mathcal{H}_0^{\varsigma}(\Lambda)\to\mathcal{W}_h^0$ is presented as

$$\mathcal{A}\left(\psi-\mathcal{Q}_h^{\zeta_1,\zeta_2,0}\psi,\xi\right)=0,\quad\forall\xi\in\mathcal{W}_h^0.\tag{4.1}$$

Additionally, we introduce the distributed semi-norm $|\cdot|_{\zeta_1,\zeta_2}$ and the distributed norm $\|\cdot\|_{\zeta_1,\zeta_2}$ as follows:

$$|\psi|_{\zeta_1,\zeta_2}=\left(\left\|{}_0\mathcal{D}_x^{\zeta_1}\psi\right\|_{L^2(\Lambda)}^2+\left\|{}_0\mathcal{D}_y^{\zeta_2}\psi\right\|_{L^2(\Lambda)}^2\right)^{1/2},\quad\|\psi\|_{\zeta_1,\zeta_2}=\left(\|\psi\|_{L^2(\Lambda)}^2+|\psi|_{\zeta_1,\zeta_2}^2\right)^{1/2}.$$

Lemma 4.3. *For $\psi\in\mathcal{H}_0^{\eta_1}\cap\mathcal{H}_0^{\eta_2},0<\eta_1,\eta_2\le 1$, then there exist a positive constant κ, where we have the following estimation*

$$\|\psi\|_{\eta_1,\eta_2}\le\kappa|\psi|_{\kappa_1,\kappa_2}$$

Proof. According to Lemma 2.8, we obtain

$$\begin{aligned}\|\psi\|_{\kappa_1,\kappa_2}^2=\|\psi\|^2+\|{}_0\mathcal{D}_x^{\eta_1}\psi\|^2+\|{}_0\mathcal{D}_y^{\eta_2}\psi\|^2&\le(1+c_1)\left\|{}_0\mathcal{D}_x^{\eta_1}\psi\right\|^2+(1+c_2)\left\|{}_0\mathcal{D}_y^{\eta_2}\psi\right\|^2\\&\le c\left(\left\|{}_0\mathcal{D}_x^{\eta_1}\psi\right\|^2+\left\|{}_0\mathcal{D}_y^{\eta_2}\psi\right\|^2\right)=c|\psi|_{\eta_1,\eta_2}^2\end{aligned}$$

Theorem 4.4. *The bilinear form $\mathcal{A}(\cdot,\cdot)$ is coercive and continuous.*

Proof. Similar to theorem (3,1) in [3]. We obtain the continuity and the coercivity, by combining Lemma 2.6 and 2.8. And Lemma 4.3, respectively.

Lemma 4.5. [28] *Let $\mathcal{B}_n$ and f_n be real valued functions defined for $n\in\mathbb{N}$ and assume that $\mathcal{F}_n\ge 0$ for all $n\in\mathbb{N}$ if*

$$\mathcal{B}_n\le w_0+\sum_{s=0}^{n-1}\mathcal{F}_s\mathcal{B}_s,\quad n\in\mathbb{N},$$

where w_0 is a non-negative constant, then

$$\mathcal{B}_n\le w_0\sum_{s=0}^{n-1}\left[1+\mathcal{F}_s\right],\quad n\in\mathbb{N}$$

Lemma 4.6. [2] *Suppose e and d are real numbers with $0\le e\le d$. Then, there exists a positive constant $\mathbf{P}$, which independent on d, such that for any function ψ belonging to both $\mathcal{H}_0^e(\Lambda)$ and $\mathcal{H}^d(\Lambda)$, is verified the estimate inequality:*

$$\left\|\psi-\mathcal{Q}_h^{1,0}\psi\right\|_{\mathcal{H}^e(\Lambda)}\le\mathbf{P}h_l^{\min(d,M)-e}N^{e-d}\|\psi\|_{\mathcal{H}^d(\Lambda)}.$$

The diameters h_l of the element l verified $h \leq h_l \leq qh$ for all l, where h and q are positive constants.

Lemma 4.7. *Consider real numbers ζ, ς, and $\mathcal{L}$ satisfying $0 < \zeta, \varsigma < 1 < \mathcal{L}$, then, there exists a positive constant $\mathbf{P}$ that is independent of N such that, for any function $\psi \in \mathcal{H}_0^{\zeta}(\Lambda) \cap \mathcal{H}_0^{\varsigma}(\Lambda) \cap \mathcal{H}^{\mathcal{L}}(\Lambda)$, the following estimate holds:*

$$\|\psi - \mathcal{Q}_h^{\zeta,\varsigma,0}\psi\|_{\zeta,\varsigma} \leq \mathbf{P}\left(h_l^{\min(d,M)-\max(\zeta,\varsigma)} N^{\max(\zeta,\varsigma)-\mathcal{L}}\right)\|\psi\|_{\mathcal{H}^{\mathcal{L}}(\Lambda)}.$$

Proof. Based on Theorem 4.4, we use the V-elliptic of $\mathcal{A}$, then

$$\|\psi - \mathcal{Q}_h^{\zeta,\varsigma,0}\psi\|_{\zeta,\varsigma}^2 \leq \mathbf{P}\mathcal{A}\left(\psi - \mathcal{Q}_h^{\zeta,\varsigma,0}\psi, \psi - \mathcal{Q}_h^{\zeta,\varsigma,0}\psi\right),$$

Eq. (4.1) gives

$$\|\psi - \mathcal{Q}_h^{\zeta,\varsigma,0}\psi\|_{\zeta,\varsigma}^2 \leq \mathbf{P}\mathcal{A}\left(\psi - \mathcal{Q}_h^{\zeta,\varsigma,0}\psi, \psi - \psi_h\right), \quad \psi_h \in \mathcal{W}_h^0,$$

Replacing $\psi_h = \mathcal{Q}_h^{1,0}\psi$, using the continuity of $\mathcal{A}$, from the Theorem 4.4, then

$$\|\psi - \mathcal{Q}_h^{\zeta,\varsigma,0}\psi\|_{\zeta,\varsigma} \leq \mathbf{P}\|\psi - \mathcal{Q}_h^{\zeta,\varsigma,0}\psi\|_{\zeta,\varsigma}\|\psi - \mathcal{Q}_h^{1,0}\psi\|_{\zeta,\varsigma},$$

According to Lemma 4.3, we obtain

$$\|\psi - \mathcal{Q}_h^{\zeta,\varsigma,0}\psi\|_{\zeta,\varsigma} \leq \mathbf{P}\|\psi - \mathcal{Q}_h^{\zeta,\varsigma,0}\psi\|_{\zeta,\varsigma}\|\psi - \mathcal{Q}_h^{1,0}\psi\|_{\mathcal{H}^{\mathcal{L}}(\Lambda)},$$

Applying Lemma 4.6, we conclude

$$\|\psi - \mathcal{Q}_h^{\zeta,\varsigma,0}\psi\|_{\zeta,\varsigma} \leq \mathbf{P}\left(h_l^{\min(d,M)-\max(\zeta,\varsigma)} N^{\max(\zeta,\varsigma)-\mathcal{L}}\right)\|\psi\|_{\mathcal{H}^{\mathcal{L}}(\Lambda)}.$$

Theorem 4.8. *Let ψ be the solution of the problem (1.1), where $\psi \in \mathcal{H}_0^{\zeta_1}(\Lambda) \cap \mathcal{H}_0^{\zeta_2}(\Lambda) \cap \mathcal{H}^{\mathcal{L}}(\Lambda)$ and ψ^n be the solution of the fully discrete scheme. Then, there exists $\mathbf{P} > 0$, independent of n, Δt, and N, such that*

$$\|\mathbf{e}^n\|^2 \leq \mathbf{P}\left(\Delta t^{4-2\alpha} + N^{2\max(\zeta_1,\zeta_2)-2\mathcal{L}}\right). \tag{4.2}$$

Proof. Let $\mathcal{G}^n = \psi^n - \mathcal{Q}_h^{\zeta,\varsigma,0}\psi^n$, $\mathcal{V}^n = \mathcal{Q}_h^{\zeta,\varsigma,0}\psi^n - \bar{\psi}^n$, and $\mathbf{e}^n = \mathcal{V}^n + \mathcal{G}^n$.

Assume that $\mathbf{e}^0$=0. Using Eqs. (3.3) and (3.5), we get

$$\left(\mathcal{T}_t\psi^n, \xi\right) + \mathcal{A}\left(\psi^n, \xi\right) = \left(F^n, \xi\right) + \left(\mathfrak{R}^n, \xi\right), \quad \forall \xi \in \mathcal{W}_h^0, \tag{4.3}$$

$$\left(\mathcal{T}_t\bar{\psi}^n, \xi\right) + \mathcal{A}\left(\bar{\psi}^n, \xi\right) = \left(F^n, \xi\right), \quad \forall \xi \in \mathcal{W}_h^0, \tag{4.4}$$

Then, we have

$$\left(\mathcal{T}_t(\psi^n - \bar{\psi}), \xi\right) + \mathcal{A}\left(\psi^n - \bar{\psi}^n, \xi\right) = \left(\mathfrak{R}^n, \xi\right), \quad \forall \xi \in \mathcal{W}_h^0, \tag{4.5}$$

Using the relation (4.1), we obtain

$$\left(\mathcal{T}_t\mathcal{V}^n, \xi\right) + \mathcal{A}\left(\mathcal{V}^n, \xi\right) = \left(\mathfrak{R}_1, \xi\right) - \left(\mathcal{T}_t\mathcal{G}^n, \xi\right), \quad \forall \xi \in \mathcal{W}_h^0, \tag{4.6}$$

Replacing $\xi = \mathcal{V}^n$ and by $\mathfrak{A}\left(\mathcal{V}^n, \mathcal{V}^n\right) \geq M_a\left\|\mathcal{V}^n\right\|_{\zeta_1,\zeta_2}^2$, we can write that

$$\begin{aligned}M_a\Delta t\left\|\mathcal{V}^n\right\|_{\zeta_1,\zeta_2}^2 &\leq \Delta t\sum_{k=1}^{n}\left(\left(\mathcal{T}_t\mathcal{V}^k,\mathcal{V}^k\right)+\mathfrak{A}\left(\mathcal{V}^k,\mathcal{V}^k\right)\right)\\ &\leq \Delta t\sum_{k=1}^{n}\left|\left(\mathfrak{R}^k,\mathcal{V}^k\right)\right|+\Delta t\sum_{k=1}^{n}\left|\left(\mathcal{T}_t\mathcal{G}^k,\mathcal{V}^k\right)\right|,\end{aligned} \tag{4.7}$$

Which gives,

$$\begin{aligned}M_a\Delta t\left\|\mathcal{V}^n\right\|^2 \leq M_a\Delta t\left\|\mathcal{V}^n\right\|_{\zeta_1,\zeta_2}^2 &\leq \Delta t\sum_{k=1}^{n}\left\|\mathfrak{R}^k\right\|\left\|\mathcal{V}^k\right\|+\Delta t\sum_{k=1}^{n}\left\|\mathcal{T}_t\mathcal{G}^k\right\|\left\|\mathcal{V}^k\right\|\\ &\leq \Delta t\sum_{k=1}^{n}\left(\left\|\mathfrak{R}^k\right\|+\left\|\mathcal{T}_t\mathcal{G}^k\right\|\right)\left\|\mathcal{V}^k\right\|,\end{aligned} \tag{4.8}$$

From the Lemma 3.1, we can write

$$\left\|\mathcal{T}_t\mathcal{G}^n\right\|-\left\|\mathfrak{d}_t^\alpha\mathcal{G}^n\right\| \leq \left\|\mathcal{T}_t\mathcal{G}^n-\mathfrak{d}_t^\alpha\mathcal{G}^n\right\| \leq M\Delta t^{2-\alpha}\max_{0\leq t\leq T}\left\|\mathcal{G}_{tt}\right\|, \tag{4.9}$$

Lemma 4.7 and (4.9) lead to the following error bounds,

$$\begin{aligned}&\left\|\mathfrak{R}^n\right\| \leq M_1\Delta t^{2-\alpha}\max_{0\leq t\leq T}\left\|\psi_{tt}\right\|,\\ &\left\|\mathcal{T}_t\mathcal{G}^n\right\| \leq \left\|\mathfrak{d}_t^\alpha\mathcal{G}^n\right\|+M\Delta t^{2-\alpha}\max_{0\leq t\leq T}\left\|\mathcal{G}_{tt}\right\|\\ &\leq M_2\left(N^{\max(\zeta,\varsigma)-\mathcal{L}}\left\|\mathfrak{d}_t^\alpha\psi\left(t_n\right)\right\|_{\mathcal{H}^{\mathcal{L}}(\Lambda)}+\Delta t^{2-\alpha}\right),\end{aligned} \tag{4.10}$$

Using the estimates (4.10), (4.8) leads to

$$\begin{aligned}M_a\Delta t\left\|\mathcal{V}^n\right\|^2 &\leq \Delta t\sum_{k=1}^{n}\left(M_1\Delta t^{2-\alpha}\max_{0\leq t\leq T}\left\|\psi_{tt}\right\|+M_2\left(N^{\max(\zeta_1,\zeta_2)-\mathcal{L}}\left\|\mathfrak{d}_t^\alpha\psi\left(t_n\right)\right\|_{\mathcal{H}^{\mathcal{L}}(\Xi)}+\Delta t^{2-\alpha}\right)\right)\\ &\times\left\|\mathcal{V}^k\right\| \leq M_*\Delta t\sum_{k=1}^{n}\left(\Delta t^{2-\alpha}+\left(\Delta t^{2-\alpha}+N^{\max(\zeta_1,\zeta_2)-\mathcal{L}}\right)\right)\left\|\mathcal{V}^k\right\|\\ &\leq \Delta t^2\left(\Delta t^{2-\alpha}+N^{\max(\zeta_1,\zeta_2)-\mathcal{L}}\right)^2+M_*\Delta t\sum_{k=1}^{n}\left(\Delta t^{2-\alpha}+N^{\max(\zeta_1,\zeta_2)-\mathcal{L}}\right)\left\|\mathcal{V}^k\right\|,\end{aligned} \tag{4.11}$$

Now applying Lemma 4.5, we obtain

$$\begin{aligned}M_a\Delta t\left\|\mathcal{V}^n\right\|^2 &\leq \Delta t^2\left(\Delta t^{2-\alpha}+N^{\max(\zeta_1,\zeta_2)-\mathcal{L}}\right)^2\sum_{k=1}^{n}\left(1+\Delta tM_*\left(\Delta t^{2-\alpha}+N^{\max(\zeta_1,\zeta_2)-\mathcal{L}}\right)\right)\\ &\leq \Delta tT\left(\Delta t^{2-\alpha}+N^{\max(\zeta_1,\zeta_2)-\mathcal{L}}\right)^2+\Delta t^2TM_*\left(\Delta t^{2-\alpha}+N^{\max(\zeta_1,\zeta_2)-\mathcal{L}}\right)^3\\ &\leq \Delta tT\left(\Delta t^{2-\alpha}+N^{\max(\zeta_1,\zeta_2)-\mathcal{L}}\right)^2+\Delta tTM_*\left(\Delta t^{2-\alpha}+N^{\max(\zeta_1,\zeta_2)-\mathcal{L}}\right)^2\\ &\leq M\Delta tT\left(\Delta t^{2-\alpha}+N^{\max(\zeta_1,\zeta_2)-\mathcal{L}}\right)^2,\end{aligned} \tag{4.12}$$

According to Lemma 4.7, (4.12) gives

$$\|\mathbf{e}^n\| \leq m_q(\|\mathcal{V}^n\| + \|\mathcal{G}^n\|) \leq \mathbf{P}_1\left(\Delta t^{2-\alpha} + N^{\max(\zeta_1,\zeta_2)-\mathcal{L}}\right) + \mathbf{P}_2 N^{\max(\zeta_1,\zeta_2)-\mathcal{L}}, \tag{4.13}$$

We conclude that

$$\|\mathbf{e}^n\| \leq \mathbf{P}\left(\Delta t^{2-\alpha} + N^{\max(\zeta_1,\zeta_2)-\mathcal{L}}\right).$$

5. Numerical results

This section seeks to validate the theoretical results using Matlab software mathematical demonstrations. Our numerical analysis includes the computation of the numerical solution, the error measured in the $|\cdot|_\infty$ norm, and evaluating the convergence orders (C.O.), as follows

$$C.O = \frac{\log\left(\|\text{ error }_1\| / \|\text{ error }_2\|\right)}{\log\left(\kappa_1/\kappa_2\right)} \tag{5.1}$$

where error $= \left\|\psi^n - \bar{\psi}^n\right\|$ is the error equation, $\kappa_1 \neq \kappa_2$.

Example 5.1. Consider problem (1.1) as a 2D time-fractional diffusion model: $\psi(s,v,0) = \mathfrak{c}_{\mathfrak{I}}(s,v) = 0$, $(s,v) \in \Lambda$, with $H = L = l = 1$, $\Upsilon_1 = \Upsilon_2 = 0.75$, and $\digamma$ defined as

$$\begin{aligned}\digamma(s,v,t) &= (sv(s-1)(v-1))^{10}\frac{\Gamma(\alpha+\zeta_1+\zeta_2+1)t^{\zeta_1+\zeta_2}}{\Gamma(\zeta_1+\zeta_2+1)}\\ &+ 0.75t^{\alpha+\zeta_1+\zeta_2}\left[\sec\left(\pi\zeta_1\right)\mathfrak{W}_1(s,v,2\zeta_1) + \sec\left(\pi\zeta_2\right)\mathfrak{W}_1(s,v,2\zeta_2)\right],\end{aligned}$$

where

$$\begin{aligned}\mathfrak{W}_1(s,v,\mu) &= (\frac{\Gamma(11)}{\Gamma(11-\mu)}\left[s^{10-\mu}+(1-s)^{10-\mu}\right] - \frac{10\Gamma(12)}{\Gamma(12-\mu)}\left[s^{11-\mu}+(1-s)^{11-\mu}\right]\\ &+ \frac{45\Gamma(13)}{\Gamma(13-\mu)}\left[s^{12-\mu}+(1-s)^{12-\mu}\right] - \frac{120\Gamma(14)}{\Gamma(14-\mu)}\left[s^{13-\mu}+(1-s)^{13-\mu}\right]\\ &+ \frac{210\Gamma(15)}{\Gamma(15-\mu)}\left[s^{14-\mu}+(1-s)^{14-\mu}\right] - \frac{252\Gamma(16)}{\Gamma(16-\mu)}\left[s^{15-\mu}+(1-s)^{15-\mu}\right]\\ &+ \frac{210\Gamma(17)}{\Gamma(17-\mu)}\left[s^{16-\mu}+(1-s)^{16-\mu}\right] - \frac{120\Gamma(18)}{\Gamma(18-\mu)}\left[s^{17-\mu}+(1-s)^{17-\mu}\right]\\ &+ \frac{45\Gamma(19)}{\Gamma(19-\mu)}\left[s^{18-\mu}+(1-s)^{18-\mu}\right] - \frac{10\Gamma(20)}{\Gamma(20-\mu)}\left[s^{19-\mu}+(1-s)^{19-\mu}\right]\\ &+ \frac{\Gamma(21)}{\Gamma(21-\mu)}\left[s^{20-\mu}+(1-s)^{20-\mu}\right])v^{10}(1-v)^{10}\end{aligned}$$

We address the problem (1.1). Figure 1 presents the graphs of the numerical solution for $N = 8$, Δt= 2e-3, and $K = 10$ in $t = 0.5, 0.75$. with $T = 1$, focusing on error estimations for the case of $\alpha_1 = 0.5$, $2\zeta_1 = 2\zeta_2 = 1.2$, by considering the exact solution $\psi(s,v,t) = t^{\alpha_1+\zeta_1+\zeta_2}(sv(1-s)(1-v))^{10}$. Table 1 shows the L_∞ errors, the Convergence Order, and CPU time, for different values of K, where $N = 8$ and Δt= 2e-2. For $N = K = 6$, the table 2 presents the L_∞ errors, CPU time, showing that the G-SEM scheme achieves a temporal convergence order of $\mathcal{O}(\Delta t^{2-\alpha_1})$, consistent with Theorem 4.8, for different values of Δt. In the end,

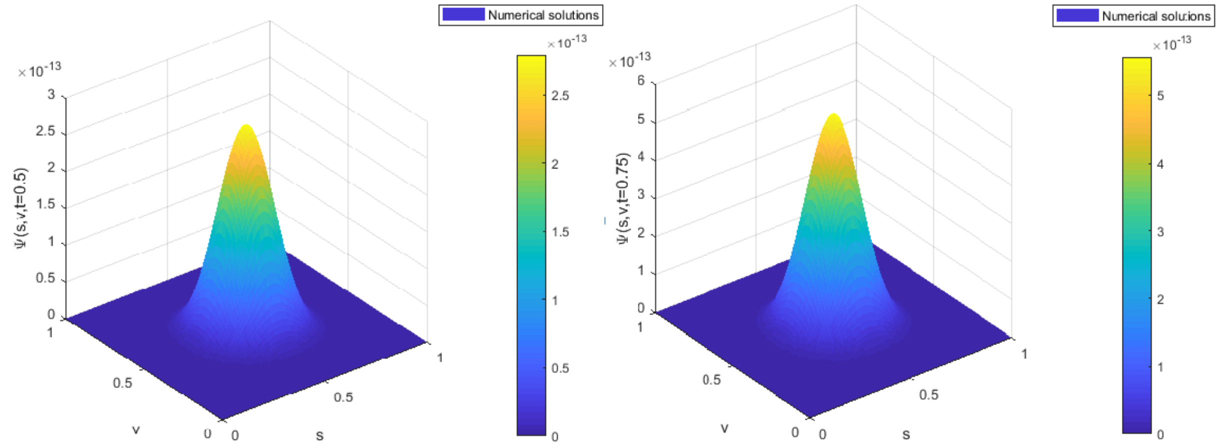

FIGURE 1. Numerical solution at time t =0.5, 0.75, with $T = 1$.

TABLE 1. L_∞ errors, C. Order and CPU for K values with $2\zeta_1 = 2\zeta_2 = 1.2$, and $\alpha_1 = 0.5$ at $T = 1$, for Ex.5.1.

K	$\left\lVert \bar{\psi}^n - \psi_n \right\rVert_\infty$	C.O	CPU (s)
2	$7.5987\mathrm{e}-05$	-	21.0155
4	$3.4897\mathrm{e}-05$	3.8955	38.1623
6	$5.5591\mathrm{e}-06$	4.7647	77.4324
8	$3.8472\mathrm{e}-06$	4.3765	85.9169
10	$4.3492\mathrm{e}-07$	6.9745	130.793

TABLE 2. L_∞ errors, C. Order and CPU for Δt values with $2\zeta_1 = 2\zeta_2 = 1.2$, and $\alpha = 0.5$ at $T = 1$ for Ex.5.1.

Δt	$\left\lVert \bar{\psi}^n - \psi_n \right\rVert_\infty$	C.O	CPU (s)
$1/100$	$3.6670e-04$	-	12.4443
$1/144$	$2.3096e-04$	1.4787	20.3657
$1/256$	$9.9803e-05$	1.4610	27.2178
$1/400$	$4.9387e-05$	1.5681	45.2592
$1/576$	$2.8828e-05$	1.4518	65.9013

TABLE 3. L_∞ errors, C. Order and CPU for N values with $2\zeta_1 = 2\zeta_2 = 1.2$, and $\alpha = 0.5$ at $T = 1$ for Ex.5.1.

N	$\left\lVert \bar{\psi}^n - \psi_n \right\rVert_\infty$	C.O	CPU (s)
3	$3.7205e-04$	-	21.1972
4	$2.2995e-05$	1.9872	36.3086
5	$5.6547e-05$	3.9607	54.7491
6	$4.8498e-06$	6.2885	83.0625
7	$6.2491e-07$	6.7012	116.183

we take K=8 and Δt= 2e-2, for different values of N, the table 3 gives the L_∞ errors, the Convergence Order, and CPU time.

Example 5.2. Consider problem (1.1) as a 2D multi-time-Riesz fractional diffusion model:

$\psi(s,v,0) = \mathfrak{c}_{\mathfrak{J}}(s,v) = 0$, $(s,v) \in \Lambda$, with $H = L = 1$, $\Upsilon_1 = \Upsilon_2 = 1$, $l = 2$, and F defined as

$$\begin{aligned} F(s,v,t) &= 100t^3\mathfrak{W}_2\left(s+\sqrt{1-v^2}, -\sqrt{1-v^2}, \zeta_1\right) + 100t^3\mathfrak{W}_2\left(\sqrt{1-v^2}-s, \sqrt{1-v^2}, \zeta_1\right) \\ &+ 100t^3\mathfrak{W}_2\left(v+\sqrt{1-s^2}, -\sqrt{1-s^2}, \zeta_2\right) + 100t^3\mathfrak{W}_2\left(\sqrt{1-s^2}-v, \sqrt{1-s^2}, \zeta_2\right) \\ &+ \frac{100\Gamma(4)}{\Gamma(4-\alpha_1)}t^{3-\alpha_1}\left(s^2+v^2-1\right)^2 + \frac{100\Gamma(4)}{\Gamma(4-\alpha_2)}t^{3-\alpha_2}\left(s^2+v^2-1\right)^2, \end{aligned}$$

where

$$\mathfrak{W}_2(s,v,\zeta) = \frac{8v^2s^{2-2\zeta}}{\Gamma(3-2\zeta)} + \frac{24vs^{3-2\zeta}}{\Gamma(4-2\zeta)} + \frac{24s^{4-2\zeta}}{\Gamma(5-2\zeta)}$$

We solve the model (1.1) with $T = 1$. Figure 2 presents the graphs of the numerical solution for $N = 8$, $\Delta t = 2e-3$, and $K = 10$ in $t = 0.5, 0.75$. Furthermore, considering the exact solution given by $\psi(s,v,t) = t^3\left(s^2+v^2-1\right)^2$, Figure 3 presents the L_∞ error with various values of N (left graph with $K = 8$ and $\Delta t = 2e-3$) and various values of K (right graph with $N = 8$ and $\Delta t = 2e-3$), in three different cases.

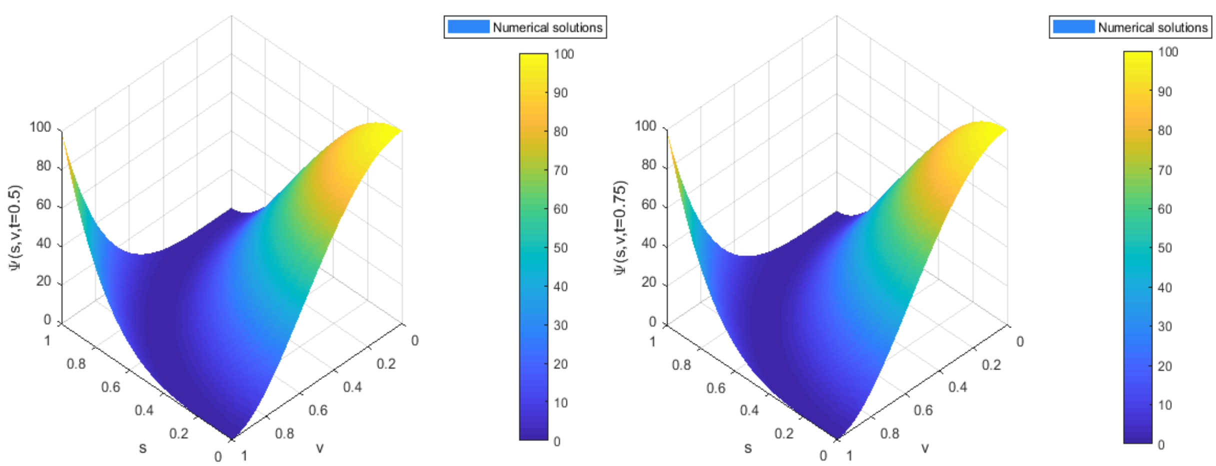

FIGURE 2. Numerical solution at time t =0.5, 0.75, with $T = 1$.

Example 5.3. Consider problem (1.1) as a time-fractional Bloch–Torrey model:

$\psi(s,v,0) = \mathfrak{c}_{\mathfrak{J}}(s,v) = 0$, $(s,v) \in \Lambda$, with $H = L = l = 1$, $\Upsilon_1 = 3$, $\Upsilon_2 = 4$, and F derived from the exact solution $\psi(s,v,t) = 10t^4(sv(1-s)(1-v))^2)$ as,

$$f(x,y,t) = 240x^2(1-x)^2y^2(1-y)^2\frac{t^{4-\alpha_1}}{\Gamma(5-\alpha_1)} + 3\mathfrak{W}_3(s,v,\zeta_1) + 4\mathfrak{W}_3(v,s,\zeta_2),$$

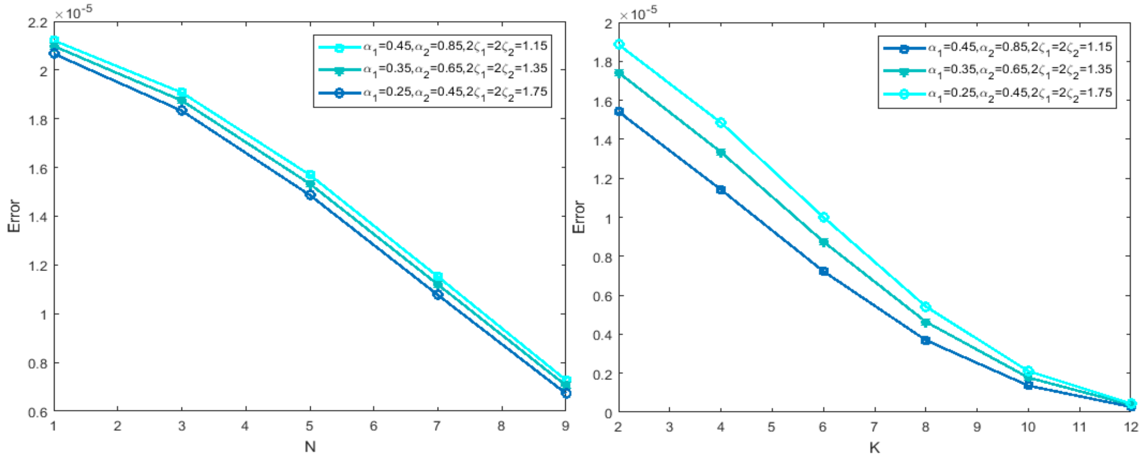

FIGURE 3. L_∞ Errors for different values of N, and K, with $T = 1$.

$$\mathfrak{W}_3(s,v,\zeta) = \frac{t^4 v^2(1-v)^2}{\cos(\zeta\pi)}$$
$$\times \left\{ \frac{s^{2-2\zeta} + (1-s)^{2-2\zeta}}{\Gamma(3-2\zeta)} - \frac{6s^{3-2\zeta} + 6(1-s)^{3-2\zeta}}{\Gamma(4-2\zeta)} + \frac{12s^{4-2\zeta} + 12(1-s)^{4-2\zeta}}{\Gamma(5-2\zeta)} \right\}.$$

TABLE 4. Comparaison of L_∞ errors, with C. Order for h values with $2\zeta_1 = 2\zeta_2 = 1.2$, and $\alpha = 0.3$, at $T = 0.5$, for Ex.5.3.

h	$\left\|\bar{\psi}^n - \psi_n\right\|_\infty$	C.O	FEM [29]	C.O
1/4	$1.0555e-04$	-	$1.4945e-04$	-
1/8	$3.9028e-05$	1.4167	$3.4586e-05$	2.1114
1/16	$2.4016e-06$	1.4223	$3.6326e-06$	2.1799
1/24	$1.2146e-06$	1.4186	$1.7790e-06$	2.1610
1/32	$1.1387e-07$	1.4129	$1.7177e-06$	2.1386

TABLE 5. Comparaison of L_∞ errors, C. Order for Δt values with $2\zeta_1 = 2\zeta_2 = 1.6$, and $\alpha = 0.6$, at $T = 0.5$, for Ex.5.3.

$\Delta t = h$	$\left\|\bar{\psi}^n - \psi_n\right\|_\infty$	C.O	FEM [29]	C.O
1/5	$1.0019e-04$	-	$1.0501e-04$	-
1/10	$1.4458e-05$	1.4289	$2.3472e-05$	2.1615
1/20	$3.4846e-06$	1.4451	$5.3245e-06$	2.1402
1/40	$8.7746e-07$	1.4223	$1.2558e-06$	2.0840
1/60	$1.1387e-07$	1.4992	$5.5859e-07$	1.9980

We solve (1.1) as a time-fractional Bloch–Torrey equation at $T = 0.5$. We put $N = 8$, and $K = 10$, Table 4 shows the effectiveness of our present method

G-SEM compared to the standard FEM, by showing the L_2 errors for different values of h, taking $\Delta t = 1/64$, for $2\zeta_1 = 2\zeta_2 = 1.2$, and $\alpha = 0.3$. In addition, Table 5 compared our present method to the FEM, by showing the L_2 errors for different values h, taking $\Delta t = h$, for $2\zeta_1 = 2\zeta_2 = 1.6$, and $\alpha_1 = 0.6$. Our method is characterized by a high order of accuracy in time and space direction compared to the technique in [29].

6. Conclusion

This study explores a numerical spectral method for a two-dimensional multi-time fractional diffusion equation. The finite difference method of order $\mathcal{O}\left(\Delta t^{2-\alpha}\right)$ was used to approximate the multi-time Caputo fractional derivative and the unconditional stability was proved of the time-discrete scheme. Further, a spectral element method was employed for the Riesz fractional derivative operators to derive a fully discrete scheme. Therefore, the error estimate was analyzed, and the spectral approach was proven to be convergent, where $\mathcal{O}\left(\Delta t^{2-\alpha} + N^{\max(\zeta_1,\zeta_2)-\mathcal{L}}\right)$ is the order of accuracy. We solved and simulated numerical problems using Matlab software to demonstrate the method's efficiency.

References

1. Baskonus, H. M., Mekkaoui, T., Hammouch, Z., & Bulut, H. (2015). Active control of a chaotic fractional order economic system. Entropy, 17(8), 5771-5783. https://doi.org/10.3390/e17085771
2. Bernardi, C., & Maday, Y. (1997). Spectral methods. Handbook of numerical analysis, 5, 209-485. https://doi.org/10.1016/S1570-8659(97)80003-8
3. Dehghan, M., & Abbaszadeh, M. (2018). An efficient technique based on finite difference/finite element method for solution of two-dimensional space/multi-time fractional Bloch–Torrey equations. Applied Numerical Mathematics, 131, 190-206. https://doi.org/10.1016/j.apnum.2018.04.009
4. Deville, M. O., Fischer, P. F., & Mund, E. H. (2002). High-order methods for incompressible fluid flow (Vol. 9). Cambridge university press. https://doi.org/10.1017/CBO9780511546792
5. El-Aqqad, B. (2024). The equations coupled by Von Karman system with thermoelasticity. Gulf Journal of Mathematics, 17(2), 190-207. https://doi.org/10.56947/gjom.v17i2.2171
6. Ervin, V. J., & Roop, J. P. (2006). Variational formulation for the stationary fractional advection dispersion equation. Numerical Methods for Partial Differential Equations: An International Journal, 22(3), 558-576. https://doi.org/10.1002/num.20112
7. Guo, T., Nikan, O., Avazzadeh, Z., & Qiu, W. (2022). Efficient alternating direction implicit numerical approaches for multi-dimensional distributed-order fractional integro differential problems. Computational and Applied Mathematics, 41(6), 236. 10.1007/s40314-022-01934-y
8. Huang, J., Nie, N., & Tang, Y. (2014). A second order finite difference-spectral method for space fractional diffusion equations. Science China Mathematics, 57, 1303-1317. -1317. https://doi.org/10.1007/BFb0058714
9. Hussain, M., & Haq, S. (2019). Weighted meshless spectral method for the solutions of multi-term time fractional advection-diffusion problems arising in heat and mass transfer. International Journal of Heat and Mass Transfer, 129, 1305-1316. https://doi.org/10.1016/j.ijheatmasstransfer.2018.10.039

10. Jiwari, R., & Kumar, N. (2023). Analysis and simulation of Korteweg-de Vries-Rosenau-regularised long-wave model via Galerkin finite element method. Computers & Mathematics with Applications, 135, 134-148. https://doi.org/10.1016/j.camwa.2023.01.027
11. Jiwari, R. (2024). A new error estimates of finite element method for (2+ 1)-dimensional nonlinear advection-diffusion model. Applied Numerical Mathematics, 198, 22-42. https://doi.org/10.1016/j.apnum.2023.12.005
12. Li, X., Mao, Z., Wang, N., Song, F., Wang, H., & Karniadakis, G. E. (2020). A fast solver for spectral elements applied to fractional differential equations using hierarchical matrix approximation. Computer Methods in Applied Mechanics and Engineering, 366, 113053. https://doi.org/10.1016/j.cma.2020.113053
13. Meerschaert, M. M., & Sikorskii, A. (2012). Stochastic Models for Fractional Calculus. https://doi.org/10.1515/9783110258165
14. Mittal, R. C., & Pandit, S. (2019). A numerical algorithm to capture spin patterns of fractional Bloch nuclear magnetic resonance flow models. Journal of Computational and Nonlinear Dynamics, 14(8), 081001. https://doi.org/10.1115/1.4043565
15. Nikan, O., Avazzadeh, Z., & Tenreiro Machado, J. A. (2024). Localized kernel-based meshless method for pricing financial options underlying fractal transmission system. Mathematical Methods in the Applied Sciences, 47(5), 3247-3260. https://doi.org/10.1002/mma.7968
16. Ortigueira, M. D. (2011). Fractional calculus for scientists and engineers (Vol. 84). Springer Science & Business Media. https://doi.org/10.1007/978-94-007-0747-4
17. Patera, A. T. (1984). A spectral element method for fluid dynamics: laminar flow in a channel expansion. Journal of computational Physics, 54(3), 468-488. https://doi.org/10.1016/0021-9991(84)90128-1
18. Podlubny, I. (1998). Fractional differential equations: an introduction to fractional derivatives, fractional differential equations, to methods of their solution and some of their applications. elsevier.
19. Quarteroni, A., & Valli, A. (2008). Numerical approximation of partial differential equations (Vol. 23). Springer Science & Business Media. https://doi.org/10.1007/978-3-540-85268-1
20. Roop, J. P. (2004). Variational solution of the fractional advection dispersion equation. Clemson University. 2004.
21. Samko, S. G. (1993). Fractional integrals and derivatives. Theory and applications.
22. Schumer, R., Meerschaert, M. M., & Baeumer, B. (2009). Fractional advection-dispersion equations for modeling transport at the Earth surface. Journal of Geophysical Research: Earth Surface, 114(F4). https://doi.org/10.1029/2008JF001246
23. Shen, J., Tang, T., & Wang, L. L. (2011). Spectral methods: algorithms, analysis and applications (Vol. 41). Springer Science & Business Media.https://doi.org/10.1007/978-3-540-71041-7
24. Shen, J. (1994). Efficient spectral-Galerkin method I. Direct solvers of second and fourth-order equations using Legendre polynomials. SIAM Journal on Scientific Computing, 15(6), 1489-1505. https://doi.org/10.1137/0915089
25. Sheng, C., & Shen, J. (2017). A hybrid spectral element method for fractional two-point boundary value problems. Numerical Mathematics: Theory, Methods and Applications, 10(2), 437-464. https://doi.org/10.4208/nmtma.2017.s11
26. Souleymane, Z., Lamien, B., Beidari, M., & Inoussa, T. (2024). Numerical simulation of pollutants transport in groundwater using deep neural networks informed by physics. Gulf Journal of Mathematics, 16(2), 337-352. https://doi.org/10.56947/gjom.v16i2.1863
27. Stynes, M., O'Riordan, E., & Gracia, J. L. (2017). Error analysis of a finite difference method on graded meshes for a time-fractional diffusion equation. SIAM Journal on Numerical Analysis, 55(2), 1057-1079. https://doi.org/10.1137/16M1082329
28. Sugiyama, S. (2006, August). Difference inequalities and their applications to stability problems. In Japan-United States Seminar on Ordinary Differential and Functional Equations:

Held in Kyoto/Japan, September 6–11, 1971 (pp. 1-15). Berlin, Heidelberg: Springer Berlin Heidelberg. https://doi.org/10.1007/BFb0058714

29. Zhao, Y., Bu, W., Zhao, X., & Tang, Y. (2017). Galerkin finite element method for two-dimensional space and time fractional Bloch–Torrey equation. Journal of Computational Physics, 350, 117-135. https://doi.org/10.1016/j.jcp.2017.08.051

[1] LaR2A, FS, Abdelmalek Essaadi University, Tetouan, Morocco
Email address: mouhssine.zakaria@etu.uae.ac.ma
Email address: moujahid.abdelaziz@uae.ac.ma